APPLICATION

Improved uniformity and anisotropy of through-mask electrochemical micromachining by localized etching and homogeneous flow

Leonie Jakob[1] · Jonas Eckert[1] · Carl Podevijn[1] · Sven Kluska[1] · Mathias Junginger[2] · Christian Ranzinger[2] · Jonas Bartsch[1]

Abstract

This contribution aims to point out the potential of through-mask electrochemical micromachining (TMEMM) as an environmentally friendly alternative for thin metal layer patterning for applications such as printed circuit boards (PCBs). Two process chamber concepts with shearing and impinging electrolyte flow, based on the concept of localized etching, are introduced. The etching results, obtained with simple mask designs, were investigated regarding homogeneity in etch depth and anisotropy. Compared to a simple setup with unspecific electrolyte flow and full area etching, a significant improvement in microscopic and macroscopic homogeneity (deviations reduced from >100 to <10%) and anisotropy (etch factors increased from ~4 to >7) could be shown. A comparison to an industrial chemical etching process using a simple mask design revealed equal macroscopic homogeneity and higher etch factors in TMEMM. Only the microscopic homogeneity leaves still room for improvement. It is presented for the first time that island formation can be prevented completely over a large area (5 × 20 mm^2) with TMEMM. These results demonstrate the advantages and the potential that can be achieved with TMEMM by designing appropriate tools.

Keywords Through-mask electrochemical micromachining · Electrolyte flow · Localized etching · Homogeneity · Island formation · Anisotropy

1 Introduction

Triggered by the climate change and the ambitious climate goals laid down in the Paris Agreement 2015, green technologies and renewable energies (e.g., photovoltaics, electromobility or batteries) will be of increasing importance in the next years. At the same time, it is very crucial to establish resource and time conserving and environmentally friendly fabrication processes in these aspiring fields.

When focusing on the patterning of thin metal layers as an important process step, the manufacturing of printed circuit boards is probably the most obvious application, related to the mentioned fields. The drilling of micro holes or the fabrication of metal masks are other possible applications.

The established patterning technique, the chemical etching, uses hazardous and environmentally critical chemicals, such as $FeCl_3$ or $CuCl_2$. The electrolyte solution must be tailored for every metal. A photomask predefines the desired structure. The process is generally isotropic in nature. The typical etch rate of 50–60 µm/min [1] is acceptable for thin metal layers (20–50 µm). However, in view of increasing metal layer thickness (up to several hundred micrometers, e.g., for power electronics [2]), the etching process becomes very time consuming. Other patterning techniques (e.g., plasma etching) can be highly anisotropic, but suffer from even lower etch rates and high process costs [3].

Through-mask electrochemical micromachining (TMEMM) [4] is an alternative metal structuring technique, which has been investigated in the past years by a few groups [5–12]. The metal layer acts as the anode in an electrochemical cell, which leads to controlled electrochemical dissolution. The desired pattern is also predefined by a resist mask on the anode. Non-hazardous and cheap chemicals, such as aqueous sodium nitrate solutions, can be used as electrolyte to etch the most common metals in thin

✉ Leonie Jakob
leonie.jakob@ise.fraunhofer.de

1 Fraunhofer Institute for Solar Energy Systems (ISE),
   Heidenhofstrasse 2, 79110 Freiburg im Breisgau, Germany

2 Contag AG, Päwesiner Weg 30, 13581, Berlin, Germany

film patterning applications (e.g., Al, Cu, Ag, Ni, Fe) [13, 14]. The machinability is determined by the standard electrode potential of the metal. In principle all metals can be machined, but in aqueous electrolytes the oxygen evolution becomes the predominant reaction, when machining noble metals [14]. Very high etching rates of more than 1 mm/min can be reached and the metal removal rate can be adjusted by the applied potential. No elevated temperatures or expensive process conditions (e.g., vacuum) are needed. These intrinsic benefits make TMEMM a resource and time efficient and environmentally friendly alternative.

Nevertheless, it is well known from literature that there are several challenges that need to be tackled, to make TMEMM an industrially feasible process [15]. One key challenge is the homogeneity of the etching. A high uniformity on the macroscopic scale, over the whole sample, as well as on the microscopic scale, within single openings or features, must be provided. The so-called island formation [16], which describes a phenomenon of electrically isolated metal residues occurring in large openings, must be avoided. Highly anisotropic etching is desired, as it enables a high density of features and steep edges.

One big influencing factor to tackle the mentioned challenges is the electrolyte flow, e.g., unspecific, shearing, or impinging electrolyte flow. Additionally, there are basically two different concepts of process management: full area etching or localized etching. The latter, meaning a sequential, linewise etching of the sample, has been introduced by Datta in the 1990s [3, 15, 17]. Transferring knowledge and tools from the related field of chemical spray etching is rather difficult, as the non-continuous spray, consisting of finely dispensed droplets, is not suitable to provide the electric connection between anode and cathode. Therefore, concepts tailored for TMEMM have to be developed.

While full area etching can in principle be faster and allows for simpler processing setups, localized etching allows providing a homogeneous and custom-shaped electrolyte flow more easily. The moving of the sample yields a moving etching front that helps to compensate for small inhomogeneities and to avoid island formation. Localized etching can easily be realized as an inline process. The required absolute currents and thus the requirements on the power supplies are much lower. An additional challenge is to avoid electric current flow on the sample outside the desired process area. The publications on TMEMM published in the recent years are mainly focused on full area etching of rather small samples [8, 9, 12].

In this contribution, we focus on the impact of different electrolyte flow conditions and especially the concept of localized etching on the homogeneity and the anisotropy of the TMEMM process. We want to point out that these factors can significantly contribute to tackle the mentioned challenges. We show the potential of TMEMM for industrial

applications, but we also clearly indicate remaining challenges and tasks. Applying an unoptimized setup with full area etching and unspecific electrolyte flow reveals the properties of the TMEMM process in its native form and sets a reference for the improvements achieved with the two introduced setups using shearing and impinging electrolyte flow and localized etching. Additionally, we compare our results to chemical spray etching, the current standard in the PCB industry.

2 Experimental

Three setups with different electrolyte flow conditions were used for the TMEMM processes in this work:

- For the full area etching with *unspecific electrolyte flow*, a beaker setup with 5 mm interelectrode distance and 1000 rpm stirring was used. An expanded metal sheet was used as cathode. The electrolyte flow conditions vary strongly between the different openings on the sample and the electrolyte flow velocity is generally very low.

- The *shearing electrolyte flow* was provided by a slotted pipe. Anode and cathode were placed on the two sides of the pipe in vertical orientation with a distance of 5.5 mm; the electrolyte flow was set to 300 L/h (mean velocity: 3.5 m/s). The process area was restricted to roughly 3.4×60 mm^2, which equals the slot width where the electrodes are in contact with the electrolyte. The shearing flow is expected to be homogeneous at the different positions on the sample, leading to an equal flow velocity at all openings. The actual flow velocity within the openings is still rather low, as the flow velocity is close to zero near the boundaries, when applying shearing flow [18].

- To provide the *impinging electrolyte flow*, a 3D-printed flat jet nozzle was applied. A slotted metal sheet, working as the cathode, was placed on top of the nozzle, providing a slot width of 620 µm. The anode was oriented horizontally with 3 mm distance to the cathode. An electrolyte flow of 390 L/h (mean velocity: 3.5 m/s) was used. The real flow velocity at the sample surface and within the anode openings is strongly increased, when using impinging electrolyte flow. Small differences or inhomogeneities in the nozzle outlet lead to larger relative differences in the actual flow velocities compared to shearing electrolyte flow.

Schematic illustrations of the three types of electrolyte flow and the setups used are shown in Fig. 1.

The cathode geometries differ strongly between the setups, especially when comparing unspecific and shearing with impinging electrolyte flow. However, this factor is negligible at the applied anode-cathode distances and

Fig. 1 Schematic illustrations of the setups used to apply unspecific (left), shearing (middle), and impinging (right) electrolyte flow. The blue arrows indicate the flow direction of the electrolyte. The green rectangles/lines mark the part of the sample that is wetted. The cathode is shown in gray. The schemes are not drawn to scale. The pictures in the bottom part display the actual setups including cathode and anode
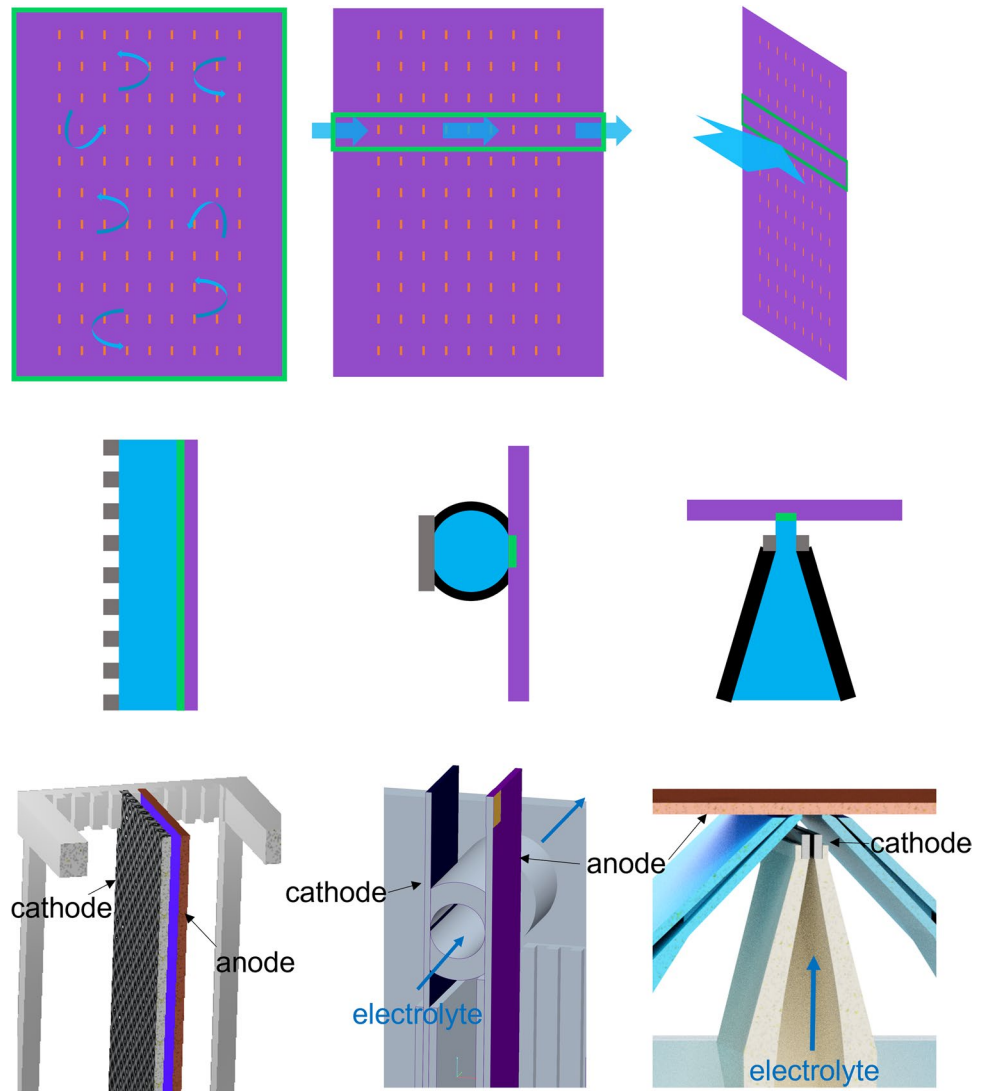
especially when compared to the influence of the electrolyte flow, which is the focus of this work.

The chemical spray etching was done at Contag AG applying the standard industrial acidic etching process. The etching solution consisted of $CuCl_2$ (120 g/L) and hydrochloric acid (115 g/L) at a constant redox potential of 560 mV (adjusted by addition of hydrogen peroxide). The temperature is maintained at 45 °C, the spray pressure was 2.3 bar, and the total etching time was 110 s.

The total sample size was 60×100 mm^2. The samples consisted of a thin copper layer mounted on an FR4 insulating substrate, partly covered by a patterned photoresist (Ordyl AM 130DI, 30 μm thick). For a first set of experiments, a simple mask design was used, as shown in Fig. 1. Ninety-nine rectangular openings with a size of 0.1×2 mm^2 are arranged in a matrix of 9×11, with a distance of 5 mm in every direction. Using this design, for all setups a current density of 40 A/cm^2 and an etching time of 4.2 s have

been used. The copper thickness was 95 μm. For the shearing and the impinging electrolyte flow, static experiments (without substrate movement) were conducted. Three rows were processed and analyzed for the two setups, whereas for the unspecific electrolyte flow three full samples were processed and three random rows (one per sample) were taken into consideration, as no systematic effect was visible on the three samples. For the chemical etching, two full samples were processed and three random rows were analyzed. This leads to an equal amount of 27 analyzed openings for every type of electrolyte flow. The characterization was done with a 3D confocal laser microscope (Olympus LEXT 4000). An area of 640×640 μm^2 in the middle of each opening was characterized. This area is horizontally divided into 16 parts of equal size. The etch depth and the etch factor are determined for every part.

For a second set of experiments, the sample design consisted of 5×20 mm^2 openings, which were etched

individually. In this case, the copper thickness was 30 μm. These samples have been processed with the unspecific (20 A/cm², 2.2 s) and the impinging electrolyte flow (20 A/cm², 35 s). In the latter case, the sample was moved across the process area with a velocity of 0.6 mm/s. By using a pressurized air blade, the process area was limited to roughly 2×60 mm². These samples were also characterized by 3D confocal microscopy.

All experiments have been conducted in a sodium nitrate electrolyte (200 g/L, pH 7, room temperature).

3 Results and discussion

The results obtained from TMEMM experiments with three different types of electrolyte flow compared to the chemical etching are presented in the following subsections. They are divided into two main sections according to the challenges of homogeneity and anisotropy.

3.1 Homogeneity

In our experiments with the full area, unspecific electrolyte flow, we encountered three main challenges concerning the homogeneity of the etching process. They are discussed separately in the following subchapters.

3.1.1 Macroscopic homogeneity

The macroscopic homogeneity, i.e., the uniformity of the etching over the whole sample, was quantified via the uniformity of the etch depth. Figure 2 displays the normalized etch depth distributions, resulting from the experiments with the three different setups and the chemical spray etching. The distribution obtained with unspecific electrolyte flow is very broad (not acceptable for any patterning process). The etch rate strongly differs in the single openings. We believe that the inhomogeneous electrolyte flow conditions explain the results at least partly, as the process is at least to some extent conducted under mass transport control. This assumption is supported by the much narrower etch depth distributions obtained with shearing and impinging electrolyte flow. Except for one outlier, all datapoints exhibit maximum 10% deviation. When comparing these results to the chemical spray etching, the conclusion can be drawn that our setups perform on the same level. Of course, it has to be emphasized that this is only valid for the simple mask design. In the final application the copper layer will be etched through, the depth uniformity is no longer directly relevant. Nevertheless, a sample exhibiting a bad depth uniformity will result in a bad width uniformity, which is of course also not acceptable.

The setup providing shearing electrolyte flow leads to a narrower distribution than the impinging electrolyte flow.
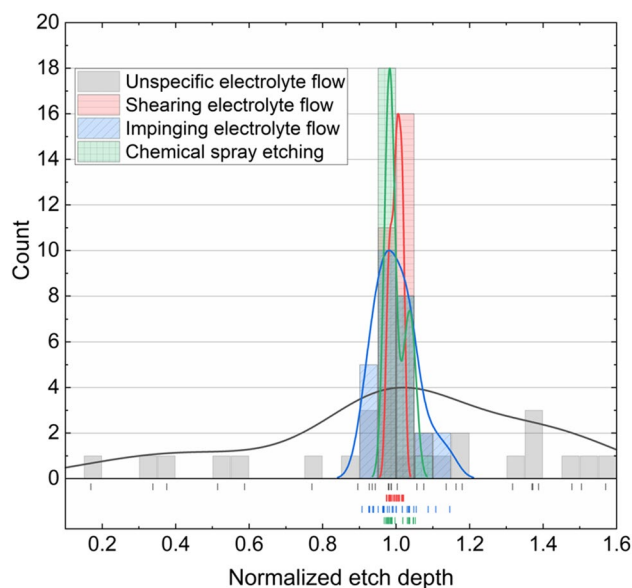

Fig. 2 Distribution of the normalized etch depth for the three different setups and the chemical etching. The normalized etch depth is the ratio of the etch depth of one trench to the mean etch depth of all analyzed trenches on the sample

This may be attributed to the fact that small differences in electrolyte velocity lead to only minor changes in local electrolyte velocity within the openings, when applying a shearing electrolyte flow. This is caused by boundary layer effects and low absolute velocities near the surface [18]. In contrast, for impinging electrolyte flow, small changes in electrolyte velocity directly influence the velocity within the openings. This leads to the conclusion that a highly homogeneous macroscopic etching is more challenging when applying impinging electrolyte flow.

3.1.2 Microscopic homogeneity

The microscopic homogeneity is analyzed via the uniformity of etching within one single opening. Figure 3 shows exemplary contour plots of etched trenches for the three setups, recorded with the 3D microscope. Dimples, meaning locally deeper etched positions, of deviating size and depth lead to a poor microscopic homogeneity in the beaker setup. Some slight dimples are still visible when applying shearing electrolyte flow, whereas none is visible with impinging electrolyte flow. The most probable explanation for the dimples is oxygen gas bubbles that are formed during the etching process. A strong gas bubble formation has been observed in the beaker setup. The gas bubbles stick to the mask openings and lead to accelerated electrolyte flow at these positions and therefore to faster etching. Due to the low mean electrolyte velocity, the bubbles are not washed away. Applying a directed and faster

Fig. 3 Exemplary contour plots recorded with the 3D microscope, displaying the qualitative differences in microscopic homogeneity between the three setups and the chemical etching. The locally deeper etched positions are indicated
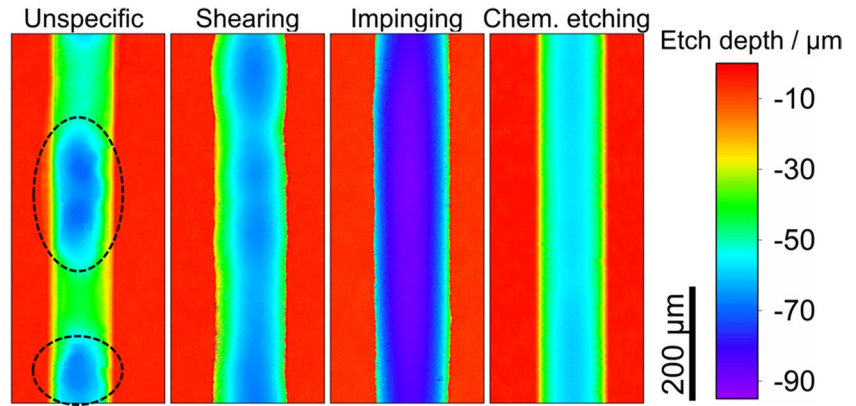
electrolyte flow helps to remove the emerging gas, avoid microscopic inhomogeneities, and increase the reproducibility. The impinging electrolyte flow leads to a significantly increased electrolyte velocity within the openings, which is most effective in washing away the gas bubbles. The etch groove obtained from chemical etching is very homogeneously etched, which can be attributed to the fundamentally homogeneous nature of chemical etching, the movement of the sample, and the absence of detrimental side reactions.

To quantify the microscopic homogeneity, 3D microscope images as shown in Fig. 3 are processed. As described earlier, each of the 3D images recorded from 27 etched grooves is divided into 16 slices. The difference between the etch depth of every slice and the mean etch depth of the groove is divided by the mean etch depth of the groove ($|(X\text{-mean}_{groove})/\text{mean}_{groove}|$). This normalized microscopic deviation is used as a measure for the microscopic homogeneity. The smaller the deviation, the better.

As it is visible from Fig. 4, the unspecific flow leads to a large scattering: For some openings, a good homogeneity is achieved, whereas other openings exhibit large deviations. This is most likely caused by varying and random influence of gas bubbles and illustrates again the low reproducibility. The scattering is strongly reduced, but still visible for the shearing and the impinging electrolyte flow. These two show an acceptable microscopic homogeneity, as most of the openings exhibit a deviation of less than 3%. The chemical etching exhibits a very good microscopic homogeneity, as already indicated by the contour plot. The deviation accounts to less than 1%.

These results show that a homogeneous and fast electrolyte flow is a prerequisite for a good microscopic homogeneity, as it reduces the influence of gas bubbles. Nevertheless, the microscopic homogeneity has to be improved to be competitive to the chemical etching. First experiments indicate that the microscopic homogeneity can be improved to roughly 1% by moving the substrate.
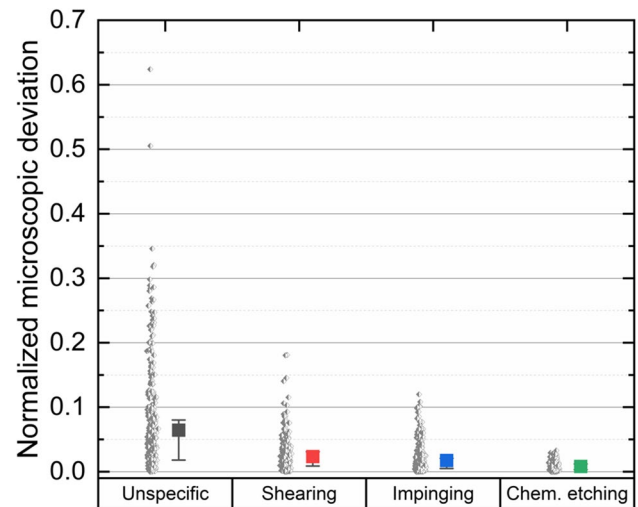

Fig. 4 Quantification of the microscopic homogeneity using a normalized microscopic deviation ($|(X\text{-mean})/\text{mean}|$). One data point displays the normalized deviation of one slice. The squares depict the mean values; the whiskers include the 25–75% range

3.1.3 Island formation

The third challenge is the island formation that occurs mainly in large, shallow openings, due to an initially faster etching at the edges of the openings [19, 20]. This is unacceptable, so solutions need to be found to avoid island formation and therefore increase the acceptance of TMEMM as a competitive process [21]. Using the sample design with the 5×20 mm^2 openings, we analyzed if the localized etching helps to avoid island formation. The principle of the moving etch front, resulting from the localized etching in combination with substrate movement, is illustrated in Fig. 5a. By ensuring a continuous connection of the etched region to the main metal layer, island formation should be prevented, when using a suitable combination of moving speed and current density.

In Fig. 5b, two exemplary openings are depicted, visualizing the beneficial effect of the moving etch front. The left
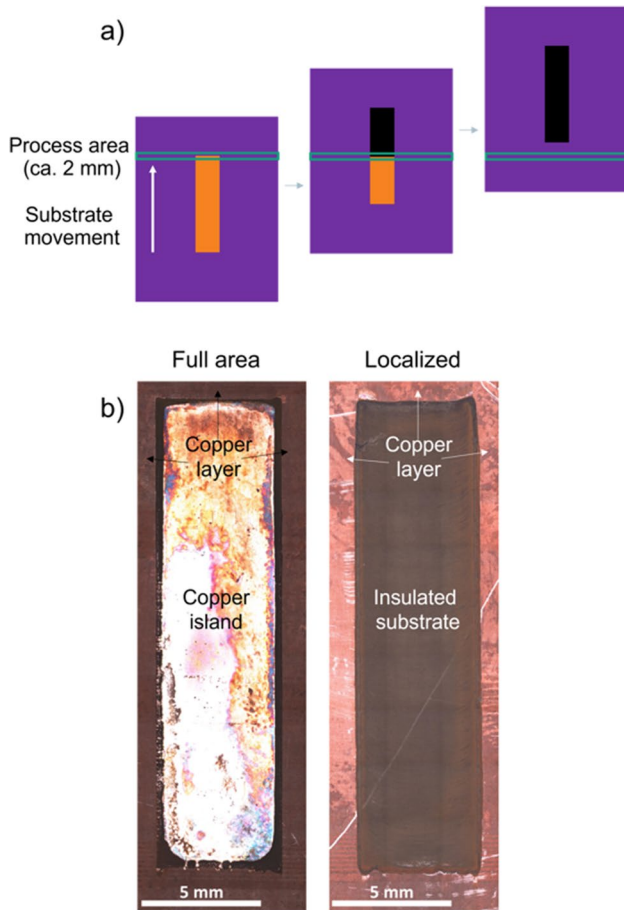
Fig. 5 a Schematic illustration of the moving etch front, as a result of localized etching in combination with substrate movement. Purple: resist mask, orange: copper, black: insulated substrate. **b** Large, shallow openings, etched with full area, unspecific electrolyte flow (left) and localized, impinging electrolyte flow (right)

Fig. 6 Etch factor values in dependence of the type of electrolyte flow and compared to chemical etching. Squares: mean values, whisker: 95% confidence interval. Inlet: schematic illustration of etch factor

microscope image (full area etching) exhibits a large metal island of roughly 15 μm height (i.e., 50% of the original metal layer thickness), which is electrically separated from the surrounding metal layer. The right image, obtained with localized etching, shows a fully etched opening. Very small metal residuals, caused by the roughness of the insulating substrate, can be removed by a short chemical post-etching step. To our knowledge, this is the first time the avoidance of island formation is demonstrated on such large areas. By applying the concept of a moving etch front, other options like the usage of dummy resist masks [4] are no longer needed.

3.2 Anisotropy

A high anisotropy is needed to enable a high density of conductive paths per area and to obtain steep edges. The so-called etch factor can be used as a measure of anisotropy. It is calculated from the ratio of etch depth to under
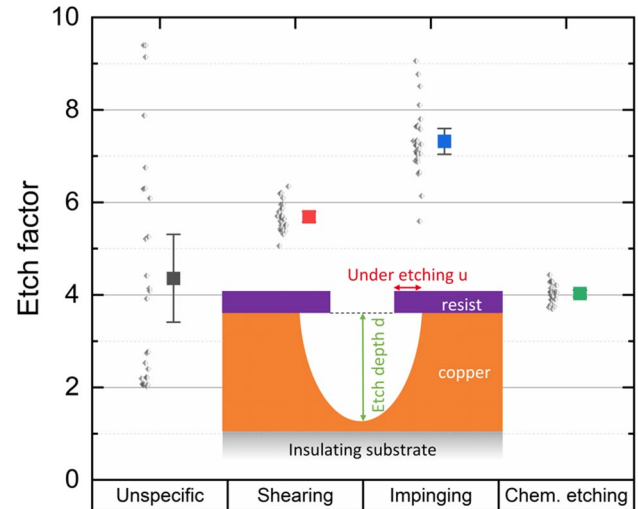
etching under the resist mask. A high etch factor is desired. The uncertainty increases by definition with increasing etch factor.

$$Etch\ factor = \frac{Etch\ depth\ d}{Under\ etching\ u} = \frac{Etch\ depth\ d}{\frac{Final\ opening\ width - Initial\ mask\ opening\ width}{2}}$$

Figure 6 shows the etch factors obtained for the different electrolyte flow conditions and for the chemical etching. A high mean etch factor of roughly 4.4 results from experiments with unspecific electrolyte flow. The single values are scattering strongly, which can most likely be attributed to the detrimental effects discussed in the previous sections, mainly the gas bubble formation. When applying a homogeneous and directed electrolyte flow, even higher etch factors of 5.7–7.3 can be obtained. As high etch factors as obtained with our setups have rarely been published before. Higher etch factors with impinging compared to shearing electrolyte flow have already been reported by Datta and Harris [15]. The mean etch factor of 4 obtained for the chemical etching indicates also a significant anisotropic etching, which can be mainly attributed to the spraying technique, as the chemical etching itself is isotropic in nature.

4 Conclusion and outlook

In this contribution, we pointed out some main challenges of TMEMM, namely, macroscopic and microscopic inhomogeneities in etch depth and island formation. All of these challenges and the entire process characteristics are strongly related to and influenced by the electrolyte flow conditions.

Full area etching with undirected flow leads to strong scattering of etch depth and etch factor, most probably due to gas bubbles adhering to the surface. The mean etch factor is reasonably high. A simple beaker setup was used in this work and no efforts were made to increase and homogenize the flow pattern for full area etching. This setup is a useful tool to demonstrate the TMEMM process in its native form and to clearly reveal the challenges, which has, to our knowledge, never been published before. The scattering might be reduced by directing a controlled and homogeneous flow onto the full area substrate. Pronounced island formation was observed, which will be hard to overcome even with improved flow conditions.

We introduced two exemplary concepts for localized etching and demonstrated that directed and homogeneous electrolyte flow, combined with the moving etching front, helps to avoid or limit the mentioned problems. With these approaches, the scattering of etch depth could be strongly reduced to 10% (macroscopic scale) and 3% (microscopic scale) deviation, which is already in an acceptable range. Nevertheless, further improvement is desirable and possible, for example, by moving the substrate. With impinging electrolyte flow, gas bubbles can be effectively removed from the reaction zone. Etch factors higher than 7 can be reached, which is much higher than the etch factors commonly published for TMEMM processes. Additional benefits, as the manifold options to individually shape the electrolyte jet, make it the most promising option at present.

The comparison to the chemical etching shows, on the simple mask design, already an almost similar level in homogeneity and a higher level of anisotropy for TMEMM on the improved setups.

For final applications, more complex patterns and larger substrates must be handled, including differently sized openings and even larger opened areas. This brings additional challenges, as inhomogeneities in current density [22, 23], alternating active areas when moving the sample and probably other entirely new challenges. Nevertheless, proving homogeneous flow conditions and homogeneous etching results on simple mask designs is an important prerequisite for transferring the process to more complex mask designs. Additionally, a concept called segmented cathode is currently under construction at Fraunhofer ISE [24]. By dividing the cathode into small segments, differences in active area can be counteracted by applying locally adapted currents. Precise current/sample speed control for an optimized status of the sample at the end of the process (as little remaining metal and as little under etching as possible) are still to be developed. Post TMEMM procedures, such as short chemical etching steps, are considered. Further challenges include the construction of industrially feasible process chambers supplying adequate limitation of the electrolyte wetting to the reaction zone and the possibility of substrate movement without negatively influencing the electrolyte jet. Also, the possibility to recover the metal from the electrolyte solution would enable an improved recycling management. A deeper and more detailed understanding of the process will help to tackle the mentioned challenges. We aim to contribute to that by further research and publications.

Declarations

Competing interests The authors declare no competing interests.

References

1. Cakir O (2006) Copper etching with cupric chloride and regeneration of waste etchant. J Mater Process Technol 175:63–68. https://doi.org/10.1016/j.jmatprotec.2005.04.024
2. Boettcher L, Karaszkiewicz S, Manessis D et al. (2012) Development of embedded power electronics modules. In: 2012 4th electronic system-integration technology conference. IEEE, pp 1–6. https://doi.org/10.1109/ESTC.2012.6542167
3. Datta M (1998) Microfabrication by electrochemical metal removal. IBM J Res Dev 42:655–670. https://doi.org/10.1147/rd.425.0655
4. Baldhoff T, Nock V, Marshall AT (2018) Review—through-mask electrochemical micromachining. J Electrochem Soc 165:E841–E855. https://doi.org/10.1149/2.1341814jes
5. Zhang X, Qu N, Li H et al (2015) Investigation of machining accuracy of micro-dimples fabricated by modified microscale pattern transfer without photolithography of substrates. Int J Adv Manuf Technol 81:1475–1485. https://doi.org/10.1007/s00170-015-7283-z
6. Chen X, Qu N, Li H et al (2015) Removal of islands from micro-dimple arrays prepared by through-mask electrochemical micromachining. Precis Eng 39:204–211. https://doi.org/10.1016/j.precisioneng.2014.09.002
7. Chen X, Qu N, Li H et al (2016) Electrochemical micromachining of micro-dimple arrays using a polydimethylsiloxane (PDMS) mask. J Mater Process Technol 229:102–110. https://doi.org/10.1016/j.jmatprotec.2015.09.008

8. Chen X, Qu N, Li H (2015) Improvement of dimensional uniformity on micro-dimple arrays generated by electrochemical micromachining with an auxiliary electrode. Int J Adv Manuf Technol 80:1577–1585. https://doi.org/10.1007/s00170-015-7147-6

9. Zhang X, Qu N, Chen X (2016) Sandwich-like electrochemical micromachining of micro-dimples. Surf Coat Technol 302:438–447. https://doi.org/10.1016/j.surfcoat.2016.05.088

10. Mahata S, Kunar S, Bhattacharyya B (2019) Fabrication of different micro patterned arrays by through mask electrochemical micromachining. J Electrochem Soc 166:E217–E225. https://doi.org/10.1149/2.0131908jes

11. Liu C-W, Chen C-H, Lee S (2021) Simulation and analysis of through-mask electrochemical machining with moving tools. Adv Mech Eng 13:168781402110099. https://doi.org/10.1177/16878140211009996

12. Singh J, Jain VK, Ramkumar J (2016) Fabrication of complex circuit on printed circuit board (PCB) using electrochemical micromachining. Int J Adv Manuf Technol 85:2073–2081. https://doi.org/10.1007/s00170-015-7817-4

13. Schneider M, Lohrengel M (2017) Electrochemical machining. In: Breitkopf C, Swider-Lyons K (eds) Springer handbook of electrochemical energy. Springer, Berlin Heidelberg, Berlin, Heidelberg, pp 941–971

14. Lohrengel MM, Rataj KP, Münninghoff T (2016) Electrochemical machining—mechanisms of anodic dissolution. Electrochim Acta 201:348–353. https://doi.org/10.1016/j.electacta.2015.12.219

15. Datta M, Harris D (1997) Electrochemical micromachining: an environmentally friendly, high speed processing technology. Electrochim Acta 42:3007–3013. https://doi.org/10.1016/S0013-4686(97)00147-3

16. Datta M (2021) Electrodissolution processes: fundamentals and applications, 1st edn. Taylor & Francis Group, Milton

17. Datta M (1995) Fabrication of an array of precision nozzles by through-mask electrochemical micromachining. J Electrochem Soc 142:3801–3805. https://doi.org/10.1149/1.2048416

18. Bergman TL, Incropera FP (2011) Fundamentals of heat and mass transfer, 7th edn. Wiley, Hoboken, NJ

19. DeBecker B, West AC (1996) Workpiece, pattern, and feature scale current distributions. J Electrochem Soc 143:486–492. https://doi.org/10.1149/1.1836469

20. Shenoy RV, Datta M, Romankiw LT (1996) Investigation of island formation during through-mask electrochemical micromachining. J Electrochem Soc 143:2305–2309. https://doi.org/10.1149/1.1836997

21. Datta M (1995) Electrochemical micromachining. Electrochem Soc Interface 4:32–35. https://doi.org/10.1149/2.F06952IF

22. Raffelstetter P, Mollay B, van den Bossche B et al (2009) Modeling strategy for predicting current density distributions on PCBs and other complex patterned substrates. J Electrochem Soc 156:D51. https://doi.org/10.1149/1.3033523

23. Raffelstetter P, Mollay B (2010) On the modeling of shape evolution in through-mask electrochemical micromachining of complex patterned substrates. Electrochim Acta 55:2149–2157. https://doi.org/10.1016/j.electacta.2009.11.049

24. Bartsch J, Kamp M, Kluska S (2020) Verfahren zur Strukturierung von Metallschichten durch elektrochemisches Abtragen(DE102020127452A1)